AIAA JOURNAL
Vol. 45, No. 6, June 2007

Modeling Scramjet Flows with Variable Turbulent Prandtl and Schmidt Numbers

X. Xiao* and H. A. Hassan†
North Carolina State University, Raleigh, North Carolina 27695-7910
and
R. A. Baurle‡
NASA Langley Research Center, Hampton, Virginia 23681-2199

DOI: 10.2514/1.26382

A complete turbulence model is presented in which the turbulent Prandtl and Schmidt numbers are calculated as part of the solution and in which averages involving chemical source terms are modeled. The model avoids the use of assumed or evolution probability distribution functions and thus results in a highly efficient algorithm for reacting flows. The predictions from the model are compared with two sets of experiments involving supersonic mixing and one involving supersonic combustion. Two sets of H_2/air chemical kinetic mechanisms are considered: one involving 7 species and 7 reactions, the other involving 9 species and 19 reactions, with reaction rates being dependent on both pressure and temperature. The results demonstrate the need for consideration of turbulence/chemistry interactions in supersonic combustion. In general, good agreement with the experiment is indicated.

Nomenclature

$C_h, C_{h1}, \ldots$	=	model constants
$C_Y, C_{Y1}, \ldots$	=	model constants
D	=	diffusion coefficient
h	=	enthalpy
k	=	turbulence kinetic energy
P	=	pressure
Pr	=	Prandtl number
Sc	=	Schmidt number
t_{ij}	=	stress tensor
u_i	=	velocity vector
Y	=	mass fraction
α	=	diffusivity
$\Delta h_{f,m}$	=	heat of formation of species m
ϵ	=	dissipation rate
ζ	=	enstrophy
λ	=	thermal conductivity
μ	=	dynamic viscosity
ν	=	kinematic viscosity
τ	=	time scale
ϕ	=	dissipation function
$\dot{\omega}$	=	production rate

Subscripts

m	=	species
t	=	turbulent

Superscripts

$''$	=	fluctuation
$\tilde{}$	=	Favre average
$\bar{}$	=	time average

Presented as Paper 0128 at the 44th AIAA Sciences Meeting and Exhibit, Reno, NV, 9–12 January 2006; received 7 July 2006; revision received 3 December 2006; accepted for publication 29 January 2007.

*Research Assistant Professor, Mechanical and Aerospace Engineering. Member AIAA.
†Professor, Mechanical and Aerospace Engineering. Fellow AIAA.
‡Aerospace Engineer, Hypersonic Airbreathing Propulsion Branch. Senior Member AIAA.

I. Introduction

ACCURATE prediction of flows in scramjet engines requires the development of turbulence models that calculate the turbulent Prandtl Pr_t and Schmidt Sc_t numbers as part of the solution and that also account for turbulence/chemistry interactions. Traditional turbulence models that only address velocity fluctuations have no mechanism for incorporating turbulence/chemistry interaction and require the specification of both Pr_t and Sc_t. Such numbers have a profound influence on flow predictions: a low value of Sc_t can result in engine unstart, whereas a higher value may result in flame blowout [1]. On the other hand, Pr_t has an important effect on mixing at high-speed flows. It is shown in [2], in which the role of variable turbulent Schmidt number on the mixing of supersonic streams was considered, that a value of $Pr_t = 0.9$ gave the best fit for data from the experiment of Cutler et al. [3], whereas a value of 0.5 gave the best fit for the experiment of Burrows and Kurkov [4].

In an attempt to address this problem, a series of step-by-step investigations were carried out to develop a model that calculates Pr_t and Sc_t as part of the solution and addresses turbulence/chemistry interactions. In [2], the role of variable Sc_t on supersonic mixing was considered, and in [5], the role of variable Pr_t on heat flux in the presence of shock wave/boundary interactions was examined. In a more recent investigation [6], the variable Sc_t formulation of [2] was extended to address reacting flows, while assuming a fixed Pr_t.

The turbulence/chemistry interaction in [6] was studied using the multivariate β PDF for mass fractions developed by Girimaji [7]. A comparison of assumed and evolution PDFs in flows involving supersonic combustion by Baurle et al. [8] showed that both formulations yielded comparable mean flow predictions. However, assumed PDFs were unable to predict higher-order correlations, such as terms involving chemical production source terms, with any reasonable accuracy. Similar results were encountered in [6]. It is shown there that the use of Girimaji's PDF has a highly dissipative effect on the concentration variance, resulting in poor agreement with measurements. Computations employing evolution PDFs are time-consuming and require excessive storage. Because of this, all higher-order terms involving the chemical production rate are modeled in this work.

To demonstrate that the modeling is not limited to one set of chemical kinetic mechanisms, two completely distinct H_2/air mechanisms are considered. The first is the seven-species/seven-

reactions mechanism developed by Jachimowski [9]. In this mechanism, all reaction rates are functions of temperature. The second is the 9-species/19-reactions mechanism developed by Connaire et al. [10]. In this mechanism, the reaction rates are both pressure- and temperature-dependent. This model was developed for combustion over a temperature range of 298–2700 K, a pressure range of 0.01–87 atm, and equivalence ratios from 0.2–6.

The present work is quite different from that of Brinckman et al. [11] and Calhoon et al. [12]. In these works, the variance of temperature/enthalpy/internal energy and its dissipation rate are based on the incompressible energy equation, which is not well suited for high-speed or reacting flows. Instead of deriving an equation for the variance of concentrations and its dissipation rate, they based their approach on an equation for the mixture fraction and its dissipation rate. Thus, the preceding approaches do not provide for turbulence/chemistry interaction and cannot be used to calculate concentrations of the various species present.

The current model is used to predict the flows in two sets of mixing experiments [3,4] and in the reacting experiment of [4]. Predictions of mass fractions and flow properties are presented and compared with the experiment; in general, good agreement is indicated.

II. Formulation of Problem

A. Governing Equations

The variable Pr_t and Sc_t formulation developed in this work requires equations for the variance of enthalpy and its dissipation rate and for the variance of concentrations and its dissipation rate. These equations were derived in [2,5] for nonreacting flows. The formulation of [2] was extended in [6] to reacting flows, while keeping Pr_t constant.

The approach that has been used to derive the final set of equations for variable Pr_t and Sc_t in the presence of reactions follows the same procedure used in [2,5,6,13]. This entails deriving the exact equations that govern the variances of concentrations and enthalpy and their dissipation rates from the Navier–Stokes equations and modeling the resulting equations term by term. Dimensional and tensorial consistency, Galilean invariance, coordinate system independence, and absence of wall or damping functions characterize the resulting set of equations, which are given in the Appendix.

The underlying turbulence model is the k-ζ model [13], where k is the variance of velocity or turbulence kinetic energy per unit mass, and ζ is the variance of vorticity or enstrophy. The final model is developed in a modular fashion and can be used in the absence or presence of reactions or for constant or variable Prandtl and/or Schmidt numbers. Thus, it can be used in any combination desired to match the physics of the problem being addressed, without having to adjust the model constants.

The procedure used in developing model equations and constants was based on the same procedure used in developing the k-ζ model [13]. Thus, the model constants were arrived at by first meeting the requirements of the log-law region and then using numerical optimization in conjunction with available experiments. Because the k-ζ model equations are tensorially consistent, Galilean-invariant, and coordinate-system-independent, the resulting model constants were used for 2-D/axisymmetric and 3-D flows, without any adjustment. It is expected that the variable Pr_t/Sc_t model presented here will function in the same manner.

The variance of the enthalpy $\widetilde{h''^2}$ and its dissipation rate ϵ_h provide an expression for the turbulent diffusivity α_t, in the form

$$\alpha_t = 0.5(C_h k \tau_h + \nu_t/\beta_h) \tag{1}$$

where

$$\tau_h = \widetilde{h''^2}/\epsilon_h, \qquad \epsilon_h = \overline{\alpha\left(\frac{\partial h''}{\partial x_i}\right)^2} \tag{2}$$

and ν_t is the turbulent eddy viscosity

$$\nu_t = C_\mu \frac{k^2}{\nu\zeta}, \qquad C_\mu = 0.09 \tag{3}$$

where C_μ and C_h are model constants, α is the laminar diffusivity, and ν is the molecular kinematic viscosity. The parameter β_h is chosen here as 0.5. The turbulent Prandtl number Pr_t is given by

$$Pr_t = \nu_t/\alpha_t \tag{4}$$

Similarly, the variance of concentrations σ_Y

$$\sigma_Y = \sum \widetilde{Y_m''^2} \tag{5}$$

and its dissipation rate ϵ_Y

$$\epsilon_Y = \sum \overline{D\left(\frac{\partial Y_m''}{\partial x_i}\right)^2} \tag{6}$$

yield the turbulent diffusion coefficient D_t as

$$D_t = 0.5(C_Y k \tau_Y + \nu_t/\beta_Y) \tag{7}$$

where

$$\tau_Y = \sigma_Y/\epsilon_Y \tag{8}$$

C_Y and β_Y are model constants, and D is the molecular diffusion coefficient. The turbulent Schmidt number Sc_t is defined as

$$Sc_t = \nu_t/D_t \tag{9}$$

Equations (1) and (8) are coded such that for constant turbulent Prandtl and/or Schmidt number calculations, one chooses β_h and/or β_Y to match the number(s) chosen. Both C_Y and C_h were obtained from Launder [14].

B. Turbulence/Chemistry Interaction

The equation for mass fraction variance σ_Y contains the term

$$\overline{Y_m''\dot{\omega}_m}$$

where Y_m'' is the fluctuation of the mass fraction of species m, and $\dot{\omega}_m$ is its mass production rate. Similarly, the equation that governs the enthalpy variance contains the term

$$\overline{h''\dot{\omega}_m \Delta h_{f,m}}$$

Table 1 Model constants for σ_Y and ϵ_Y equations

C_Y	$C_{Y,1}$	$C_{Y,2}$	$C_{Y,3}$	$C_{Y,41}$	$C_{Y,42}$	$C_{Y,5}$	$C_{Y,6}$	$C_{Y,7}$	$C_{Y,8}$	$C_{Y,9}$	$C_{Y,p}$	β_Y
0.065	1.0	0.095	−0.025	0.45	−1.0	1.0	0.5	0.78125	0.4	4.4	−0.1	0.5

Table 2 Model constants for $\widetilde{h''^2}$ and ϵ_h equations

C_h	$C_{h,2}$	$C_{h,4}$	$C_{h,5}$	$C_{h,6}$	$C_{h,7}$	$C_{h,8}$	$C_{h,9}$	$C_{h,10}$	$C_{h,11}$	$C_{h,12}$	$C_{h,13}$	β_h
0.0648	0.5	−0.4	−0.05	−0.12	1.45	0.7597	0.87	0.25	0.55	−0.86	−5.0	0.5

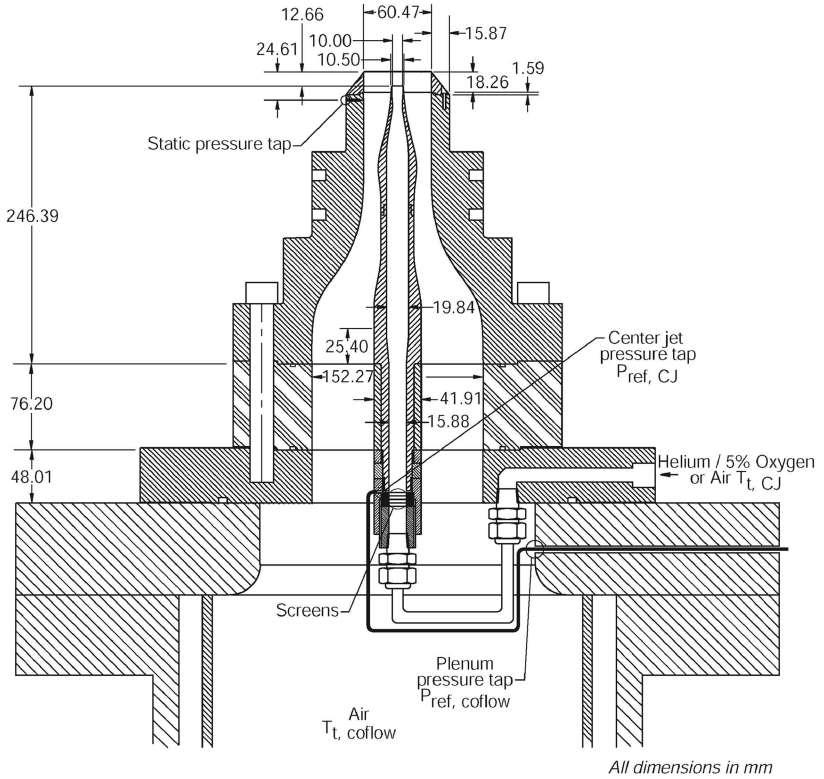

Fig. 1 Schematic of the experiment setup [3].

where h'' is the enthalpy fluctuation and $\Delta h_{f,m}$ is the heat of formation of species m.

Traditionally, the preceding terms are evaluated by using assumed or evolution PDFs or are ignored completely. The assumed PDFs are usually a product of Girimaji's [7] multivariate β PDF for mass fraction fluctuations and a Maxwellian for temperature fluctuations. Comparisons of the predictions of assumed and evolution PDFs have been conducted by Baurle et al. [8] on supersonic combustion of parallel fuel/air streams. It was shown there that both formulations give comparable mean values. However, assumed PDFs were unable to produce the correct values of the higher-order correlations. In particular, they gave the wrong sign for correlations involving mass production rates. This is why, in the absence of evolution PDFs, better predictions are obtained when the preceding correlations involving mass production rates are set to zero.

As will be shown in the Results and Discussion section, setting correlations involving mass production rate to zero is not an option for the current formulation. Because evolution PDFs require an excessive amount of computing time and storage, these terms are modeled here. Thus,

$$2\sum_m \overline{Y_m''\dot{\omega}_m} = C_{Y,8}\sum_m \sqrt{\widetilde{Y''^2}}\,\bar{\dot{\omega}}_m \tag{10}$$

and

$$\sum_m \overline{h''\dot{\omega}_m \Delta h_{f,m}} = C_{h,12}\sqrt{\widetilde{h''^2}}\sum_m \bar{\dot{\omega}}_m \Delta h_{f,m} \tag{11}$$

where $C_{Y,8}$ and $C_{h,12}$ are model constants.

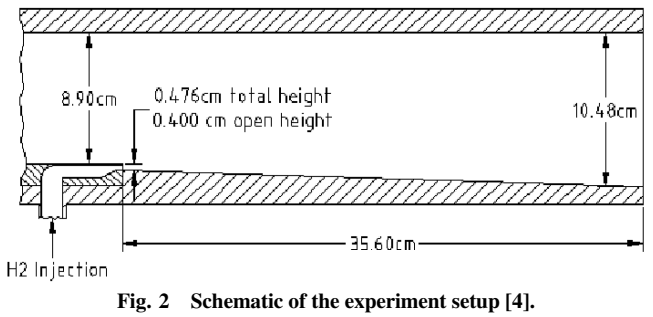

Fig. 2 Schematic of the experiment setup [4].

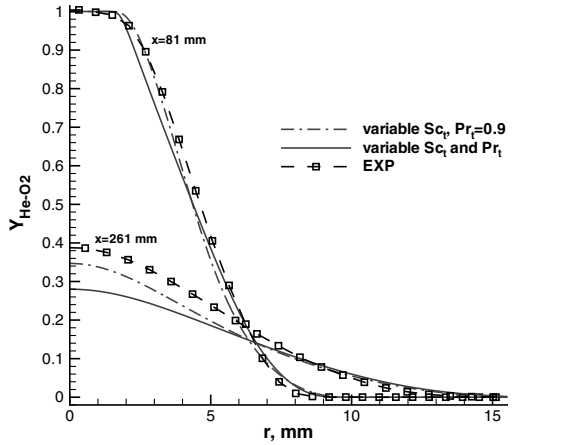

Fig. 3 Comparison of the computed and measured $He–O_2$ mass fraction [3].

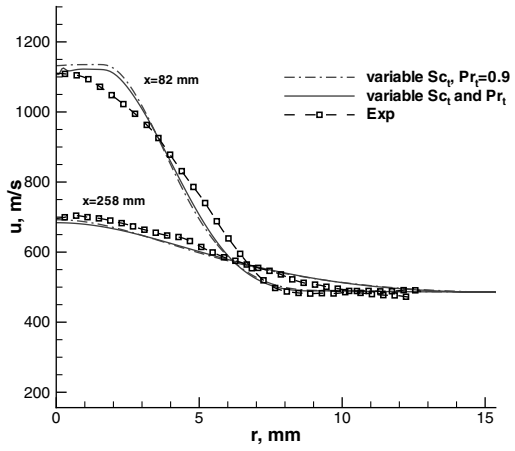

Fig. 4 Comparison of the computed and measured velocities [3].

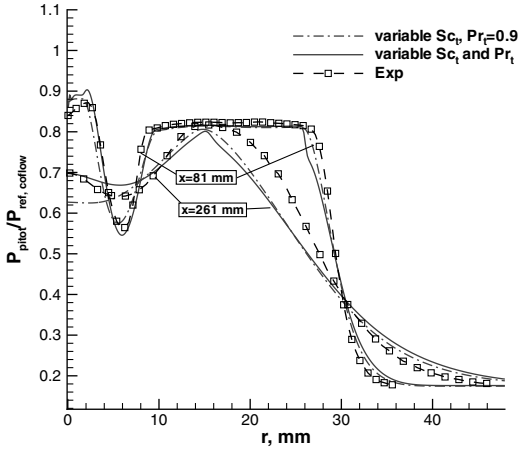

Fig. 5 Comparison of the computed and measured pitot pressure [3].

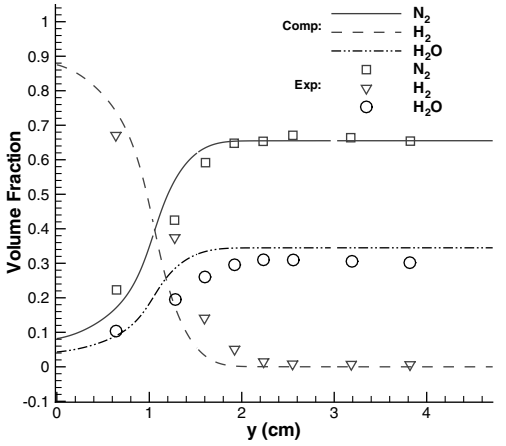

Fig. 7 Comparison of the computed and measured volume fractions [4], mixing case.

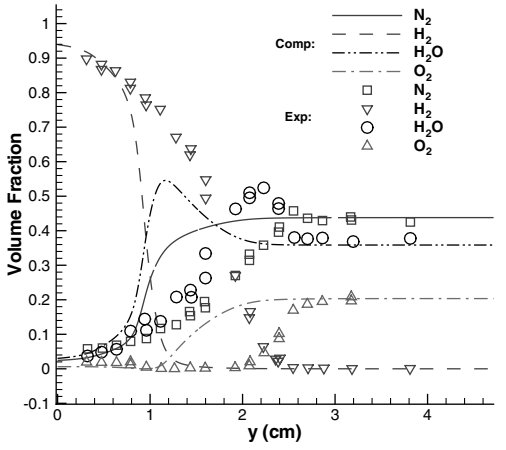

Fig. 8 Comparison of the computed and measured volume fractions [4], reacting case, in the absence of chemistry/turbulence interactions, seven species and seven reactions.

The preceding modeling is motivated by application of the mean value theorem to the indicated correlations. The modeling is dimensionally consistent. Moreover, in the absence of reactions, the resulting term is zero.

C. Numerical Procedure

A modification of REACTMB [15], a code that has been under development at North Carolina State University over the last several years, is employed in this investigation. It is a general-purpose parallel Navier–Stokes solver for multicomponent multiphase reactive flows at all speeds. It employs a second-order, essentially nonoscillatory (ENO), total-variation-diminishing (TVD) upwind method based on the low-diffusion, flux-splitting scheme of Edwards [16] to discretize the inviscid fluxes, whereas central differences are employed for the viscous and diffusion terms. Planar relaxation is employed, and the code is parallelized using domain decomposition and message passing (MPI) strategies.

D. Model Constants

The model constants developed in [2,5,6] remain unchanged. The final set of model constants are summarized in Table 1 for concentration variance and its dissipation rate and in Table 2 for enthalpy variance and its dissipation rate.

III. Results and Discussion

A theory that is developed to predict Pr_t and Sc_t as part of the solution should apply for both reacting and nonreacting flows. Because of this, the present theory is validated by two sets of experiments involving supersonic mixing [3,4] and by one experiment involving supersonic combustion [4]. In the experiment of Cutler et al. [3], a coaxial nozzle was designed to produce two uniform coaxial jets at exit. The center jet consists of 95% He and 5% O_2 by volume at a Mach number of $M = 1.8$, and the outer jet is air at $M = 1.8$. A schematic of the experiment is shown in Fig. 1. The grids employed are those used in [2,3]. The fine grid consists of 188,080 cells and is decomposed into 13 blocks for parallel computing, whereas the intermediate grid deletes every other point in the axial direction. All results employed here model the flow in the nozzle, employ the fine grid, and use the axisymmetric version of REACTMB.

The second set of experiments are those of Burrows and Kurkov [4]. A schematic of the experiment is shown in Fig. 2. Hydrogen is injected into the test section through a nickel injector parallel to the vitiated main flow. The mixing case employed nitrogen in place of air for the main flow. At the entrance of the test section, $M = 2.44$, the

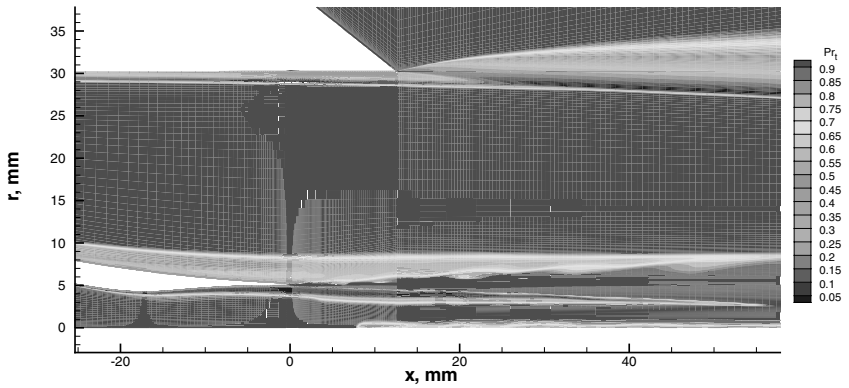

Fig. 6 Contour plot of the turbulent Prandtl number [3].

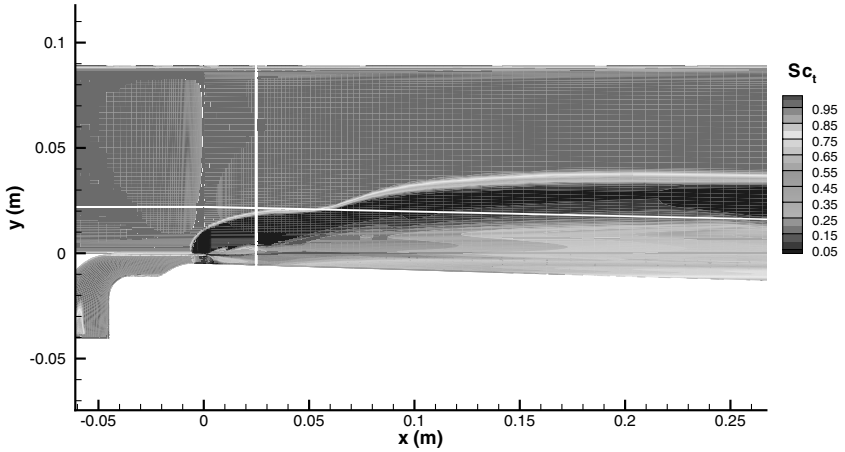

Fig. 9 Schmidt number contours, reacting case, in the absence of chemistry/turbulence interactions, seven species and seven reactions.

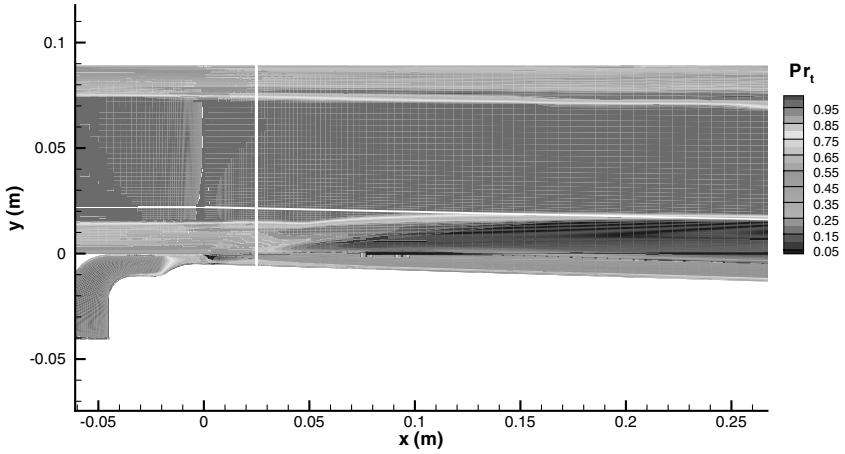

Fig. 10 Prandtl number contours, reacting case, in the absence of chemistry/turbulence interactions, seven species and seven reactions.

static pressure is 1 atm, and the static temperature is in the range of 1250–1270 K for the reacting case and about 1150 K for the mixing case. In both cases, hydrogen was injected at $M = 1$, matched pressure, and had a total temperature slightly above the ambient temperature. The two grids that are employed here are those used in [6]. Each grid consists of 15 blocks. The first grid has 86,643 cells and the second has 104,428 cells. The fine grid reflects grid refinement in the blocks in which mixing of the two streams takes place. Rather than using measured conditions at the inlet of the test section, the flows in both hydrogen and the nitrogen/air nozzle were computed. It was necessary to iterate on inflow conditions of both nozzles to arrive at the stipulated conditions at the exit of each nozzle. All results presented here employed the fine grid.

In [2], calculations of the Cutler et al. [3] experiments employed a variable Sc_t and a $Pr_t = 0.9$. Results are presented in Figs. 3–5, which compare predictions of current theory at selected stations with those of [2] and the experiment. As is seen from Fig. 3, the results of [2] for mass fraction of He at $x = 261$ mm are better than the current prediction. Figures 4 and 5 show that predictions for velocity and pitot pressure are comparable. Figure 6 shows the turbulent Prandtl contours. As is seen from Fig. 6, Pr_t is less than the background value in the regions in which mixing and reaction take place.

Figure 7 shows a comparison of volume fraction prediction with the mixing experiment of [4]. All comparisons involving mixing and combustion cases are made at the test section exit plane, which is 35.6 cm downstream from the hydrogen injection step. As is seen from the figure, good agreement is indicated. Similar results were obtained in [6].

Three sets of figures are presented for the reacting case of [4]. For the first two sets, the seven-species/ seven-reaction H_2/air model used in [6], which was originally developed by Jachimowski [9], is employed. In the first, terms involving averages of chemical source terms [Eqs. (10) and (11)] are ignored, whereas in the second, the contributions of these terms are included. As is seen from Fig. 8, poor agreement with the experiment is indicated when the correlations that involve averages of the chemical source terms are neglected. Figures 9 and 10 show the contours of Sc_t and Pr_t. It appears that the main cause of the discrepancy is a result of a reduced Pr_t near the mixing region. This has the tendency of promoting heat transfer and early combustion. Figure 11 shows that when the contributions of the

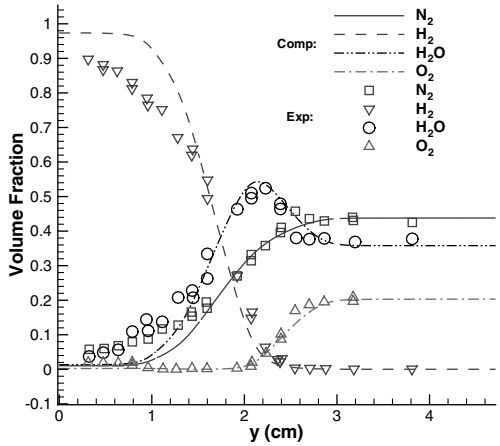

Fig. 11 Comparison of the computed and measured volume fractions [4], reacting case, in the presence of chemistry/turbulence interactions, seven species and seven reactions.

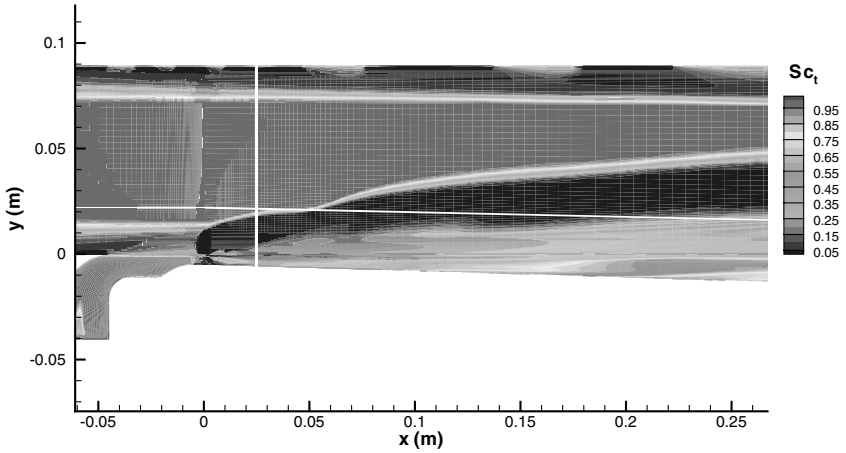

Fig. 12 Schmidt number contours, reacting case, in the presence of chemistry/turbulence interactions, seven species and seven reactions.

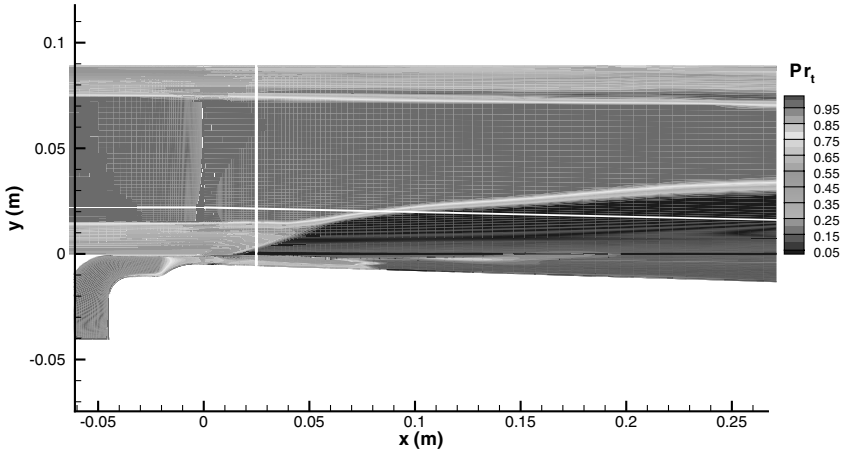

Fig. 13 Prandtl number contours, reacting case, in the presence of chemistry/turbulence interactions, seven species and seven reactions.

chemical source terms are included, much better agreement with the experiment is indicated. Figures 12 and 13 show contours of Sc_t and Pr_t, respectively. As may be seen from these figures, the Lewis number, which is the ratio of Sc_t to Pr_t, is not constant.

In the third set, Figs. 14–16 show the predictions of the 9-species/19-reactions mechanism of [10]. As is seen from Fig. 14, good agreement with experiment is indicated. This suggests that modeling approaches can serve as a substitute for approaches employing evolution PDFs. The differences in the Sc_t contours of Figs. 12 and 15 illustrate the fact that in regions in which mixing does not play a role, the value of the diffusion coefficient has little influence on the final results. Here again, examination of Figs. 15 and 16 shows that the Lewis number is not constant.

Based on the preceding results, two relevant observations can be made. First, the modeling of averages of terms involving chemical source terms is a viable option. When this approach is compared with approaches requiring assumed or evolution PDFs, a great deal of computational efficiency is achieved. Second, a relatively inexpensive calculation of variable Pr_t and Sc_t can be obtained by assuming a value for the Lewis number and eliminating either the equations for enthalpy variance and its dissipation rate or eliminating those for the variance of concentrations and its dissipation rate. This, however, will result in ignoring one of the averages involving chemical source terms. Because inclusion of such terms is important, assuming a constant Lewis number is not recommended.

IV. Conclusions

A complete turbulence model was presented in which both Pr_t and Sc_t are calculated as part of the solution and in which averages of terms involving chemical source terms are modeled. Thus, calculations of turbulent flows become similar to those of laminar flows in the sense that all that is required is the specification of initial and boundary conditions. Because the resulting algorithm does not require the use of assumed or evolution PDFs, it is computationally efficient, especially when one deals with complex three-dimensional geometries characteristics of proposed scramjet designs. The resulting algorithm, which is based on the exact Navier–Stokes equations, is dimensionally and tensorially consistent, Galilean-invariant, coordinate-system-independent, and free of damping and wall functions. Although the algorithm is applied to relatively simple

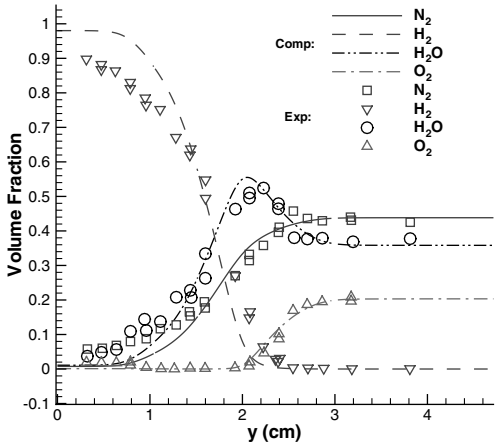

Fig. 14 Comparison of the computed and measured volume fractions [4], reacting case, in the presence of chemistry/turbulence interactions, 9 species and 19 reactions.

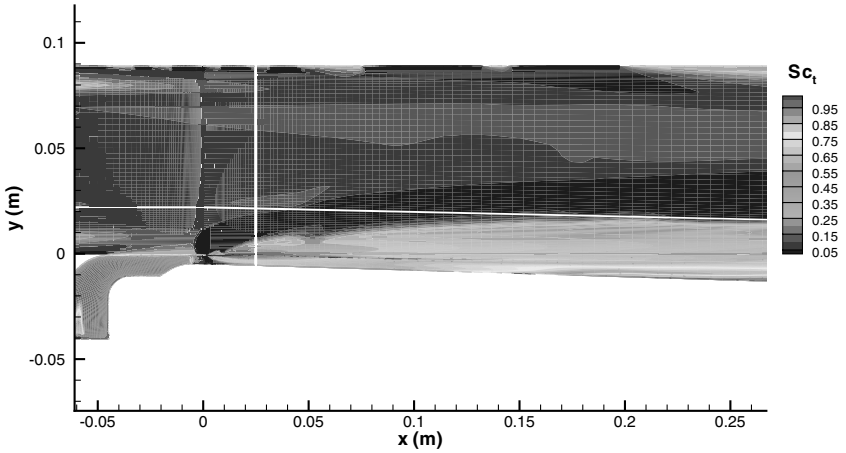

Fig. 15 Schmidt number contours, reacting case, in the presence of chemistry/turbulence interactions, 9 species and 19 reactions.

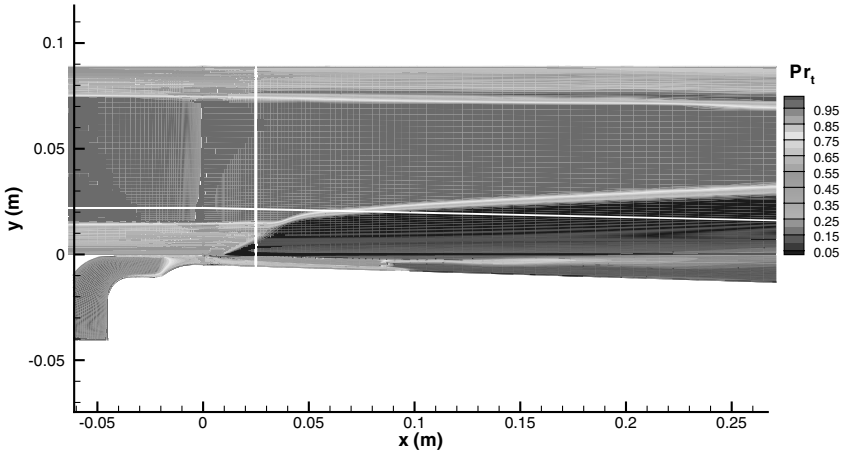

Fig. 16 Prandtl number contours, reacting case, in the presence of chemistry/turbulence interactions, 9 species and 19 reactions.

geometries, past experiences with the k-ζ model suggest that such an approach works well for complicated geometries without having to adjust any of the model constants.

Finally, correlations involving chemical source terms are important, because they account for turbulence/chemistry interactions and should always be included in combustion calculations.

Appendix: Model Equations

The Favre-averaged species conservation equations can be written as

$$\frac{\partial}{\partial t}(\bar{\rho}\tilde{Y}_m) + \frac{\partial}{\partial x_j}(\bar{\rho}\tilde{u}_j\tilde{Y}_m) = \frac{\partial}{\partial x_j}\left(\bar{\rho}D\frac{\partial \tilde{Y}_m}{\partial x_j} - \bar{\rho}\,\widetilde{Y_m''u_j''}\right) + \bar{\dot{\omega}}_m \quad \text{(A1)}$$

where

$$-\bar{\rho}\,\widetilde{Y_m''u_j''} = \bar{\rho}D_t\frac{\partial \tilde{Y}_m}{\partial x_j} \quad \text{(A2)}$$

$\bar{\rho}$ is the density, $\tilde{Y}_m$ is the mass fraction of species m, $\tilde{u}_i$ is the velocity, D is the laminar diffusion coefficient, and D_t is the turbulent diffusion coefficient.

The variance of mass fractions σ_Y is defined as

$$\sigma_Y = \sum_m \widetilde{Y_m''^2} \quad \text{(A3)}$$

and its dissipation rate ϵ_Y is defined as

$$\bar{\rho}\epsilon_Y = \overline{\sum_m \rho D\left(\frac{\partial Y_m''}{\partial x_j}\right)^2} \quad \text{(A4)}$$

The σ_Y equation is given as

$$\frac{\partial}{\partial t}(\bar{\rho}\sigma_Y) + \frac{\partial}{\partial x_j}(\bar{\rho}\tilde{u}_j\sigma_Y) = \frac{\partial}{\partial x_j}\left[\bar{\rho}(D + C_{Y,1}D_t)\frac{\partial \sigma_Y}{\partial x_j}\right] + 2\sum_m \bar{\rho}\,D_t\left(\frac{\partial \tilde{Y}_m}{\partial x_j}\right)^2 - 2\bar{\rho}\epsilon_Y + 2\sum_m \overline{\dot{\omega}_m Y_m''} \quad \text{(A5)}$$

where

$$\tau_Y = \frac{\sigma_Y}{\epsilon_Y} \qquad D_t = \frac{1}{2}\left(C_Y\frac{k\sigma_Y}{\epsilon_Y} + \frac{\nu_t}{\beta_Y}\right), \qquad k = \frac{1}{2}\widetilde{u_i''u_i''}$$

$$\nu_t = C_\mu\frac{k^2}{\nu\zeta} \qquad 2\sum_m \overline{\dot{\omega}_m Y_m''} = C_{Y,8}\sum_m \sqrt{\widetilde{Y_m''^2}}\,\bar{\dot{\omega}}_m$$

$\bar{P}$ is the pressure, ν_t is the turbulent kinematic viscosity, k is the turbulent kinetic energy per unit mass and ζ is the enstrophy.

The ϵ_Y equation is given as

$$\frac{\partial}{\partial t}(\bar{\rho}\epsilon_Y) + \frac{\partial}{\partial x_j}(\bar{\rho}\tilde{u}_j\epsilon_Y) = \frac{\partial}{\partial x_j}\left[\bar{\rho}(D + C_{Y,5}D_t)\frac{\partial \epsilon_Y}{\partial x_j}\right] + 2\bar{\rho}\epsilon_Y\left(\frac{1}{3}\frac{\partial \tilde{u}_i}{\partial x_i} + C_{Y,2}b_{jk}\frac{\partial \tilde{u}_j}{\partial x_k}\right) + C_{Y,3}\bar{\rho}k\sum_m \frac{\partial}{\partial x_j}\sqrt{\widetilde{Y_m''^2}}\frac{\partial \tilde{Y}_m}{\partial x_j} + \bar{\rho}DC_{Y,41}D_t\sum_m\left(\frac{\partial^2 \tilde{Y}_m}{\partial x_j \partial x_j}\right)^2 + \bar{\rho}D\frac{C_{Y,42}}{\tau_Y}\sum_m\sqrt{\widetilde{Y_m''^2}}\frac{\partial^2 \tilde{Y}_m}{\partial x_k \partial x_k} + \bar{\rho}D_t\frac{C_{Y,6}}{\tau_Y}\sum_m\left(\frac{\partial \tilde{Y}_m}{\partial x_j}\right)^2 - C_{Y,7}\bar{\rho}\frac{\epsilon_Y}{\tau_Y} + \frac{C_{Y,9}}{\tau_Y}\frac{\rho k}{P}\sum_m\sqrt{\widetilde{Y_m''^2}}\,\bar{\dot{\omega}}_m + C_{Y,p}\frac{\bar{\rho}}{\bar{P}\tau_Y}\max\left(\frac{D\bar{P}}{Dt}, 0.0\right) \tag{A6}$$

where

$$b_{jk} = \frac{\tau_{jk}}{\bar{\rho}k} + \frac{2}{3}\delta_{jk}, \qquad \tau_{jk} = -\overline{\rho u_j'' u_k''}$$

The turbulent Schmidt number is defined as

$$Sc_t = \frac{\nu_t}{D_t} \tag{A7}$$

The mean energy equation can be written as

$$\frac{\partial}{\partial t}(\bar{\rho}\,\tilde{h}) + \frac{\partial}{\partial x_j}(\bar{\rho}\tilde{u}_j\tilde{h}) = \frac{D\bar{P}}{Dt} - \frac{\partial \bar{q}_i}{\partial x_i} + \bar{\phi} - \frac{\partial}{\partial x_j}(\overline{\rho h'' u_j''}) \tag{A8}$$

where

$$\bar{q}_i = -\left(\lambda\frac{\partial \tilde{T}}{\partial x_i} + \bar{\rho}D\sum_m \tilde{h}_m\frac{\partial \tilde{Y}_m}{\partial x_i}\right)$$

$$-\overline{\rho h'' u_j''} \equiv q_{t,j} = \bar{\rho}\left(\alpha_t\frac{\partial \tilde{h}}{\partial x_j} + D_t\sum_m \tilde{h}_m\frac{\partial \tilde{Y}_m}{\partial x_j}\right)$$

$$\bar{\phi} = \bar{t}_{ij}\frac{\partial \tilde{u}_i}{\partial x_j} + \bar{\rho}\epsilon, \qquad \epsilon = \nu\zeta \qquad \bar{t}_{ij} = 2\mu\left(S_{ij} - \frac{1}{3}\delta_{ij}\frac{\partial \tilde{u}_k}{\partial x_k}\right)$$

$$S_{ij} = \frac{1}{2}\left(\frac{\partial \tilde{u}_i}{\partial x_j} + \frac{\partial \tilde{u}_j}{\partial x_i}\right)$$

$\tilde{h}$ is the enthalpy, $\bar{q}_i$ is the laminar heat flux, and α_t is the turbulent diffusivity.

The enthalpy variance ($\tilde{h}''^2$) equation can be written as

$$\frac{\partial}{\partial t}\left(\bar{\rho}\,\widetilde{h''^2}/2\right) + \frac{\partial}{\partial x_j}\left(\bar{\rho}\tilde{u}_j\widetilde{h''^2}/2\right) = \frac{\partial}{\partial x_j}\left[\bar{\rho}(\gamma\alpha + \alpha_t C_{h,2})\frac{\partial \widetilde{h''^2}/2}{\partial x_j}\right] + 2\mu\gamma S_{ij}\left[\frac{\partial}{\partial x_j}\left(\frac{q_{t,i}}{\bar{\rho}}\right) + \frac{\partial}{\partial x_i}\left(\frac{q_{t,j}}{\bar{\rho}}\right)\right] - \frac{4}{3}\mu\gamma S_{kk}\frac{\partial}{\partial x_j}\left(\frac{q_{t,j}}{\bar{\rho}}\right) - (\gamma - 1)\bar{\rho}\,\widetilde{h''^2}\frac{\partial \tilde{u}_i}{\partial x_i} - q_{t,i}\frac{\partial \tilde{h}}{\partial x_i} + 2C_{h,4}\gamma\mu\sqrt{\widetilde{h''^2}}\zeta - \gamma\bar{\rho}\epsilon_h - \sum_m \overline{h''\dot{\omega}_m}\,\Delta h_{f,m} \tag{A9}$$

with

$$\gamma = C_p/C_v, \qquad \alpha_t = \frac{1}{2}\left(C_h k\tau_h + \frac{\nu_t}{\beta_h}\right), \qquad \tau_h = \frac{\widetilde{h''^2}}{\epsilon_h}$$

$$\epsilon_h = \overline{\alpha\left(\frac{\partial h''}{\partial x_i}\right)^2}, \qquad \sum_m \overline{h''\dot{\omega}_m}\,\Delta h_{f,m} = C_{h,12}\sqrt{\widetilde{h''^2}}\sum_m \bar{\dot{\omega}}_m\Delta h_{f,m}$$

where ϵ_h is the dissipation rate of the enthalpy variance, and α is the laminar diffusivity.

The equation for the dissipation rate of enthalpy variance is taken as

$$\frac{\partial}{\partial t}(\bar{\rho}\epsilon_h) + \frac{\partial}{\partial x_j}(\bar{\rho}\tilde{u}_j\epsilon_h) = -\bar{\rho}\epsilon_h\left(C_{h,5}b_{jk} - \frac{\delta_{jk}}{3}\right)\frac{\partial \tilde{u}_j}{\partial x_k} + C_{h,6}\bar{\rho}k\frac{\partial\sqrt{\widetilde{h''^2}}}{\partial x_j}\frac{\partial \tilde{h}}{\partial x_j} + \frac{\partial}{\partial x_j}\left[(\gamma\alpha + C_{h,7}\alpha_t)\frac{\partial \epsilon_h}{\partial x_j}\right]C_{h,8}\frac{q_{t,j}}{\tau_h}\frac{\partial \tilde{h}}{\partial x_j} - \gamma\bar{\rho}\epsilon_h\left(\frac{C_{h,9}}{\tau_h} + \frac{C_{h,10}}{\tau_k}\right) + C_{h,11}\epsilon_h\left[\frac{D\bar{\rho}}{Dt} + \frac{\bar{\rho}}{\bar{P}}\max\left(\frac{D\bar{P}}{Dt}, 0.0\right)\right] + \frac{C_{h,13}(\rho k/P)\sqrt{\widetilde{h''^2}}\sum_m \bar{\dot{\omega}}_m\Delta h_{f,m}}{\tau_Y + \tau_h} \tag{A10}$$

where

$$\tau_k = \frac{k}{\nu\zeta}$$

The model constants C_h and $C_{h,1\text{–}12}$ are given in Table 2. The turbulent Pr_t is defined as

$$Pr_t = \frac{\nu_t}{\alpha_t} \tag{A11}$$

Acknowledgment

We wish to express our appreciation to George Rumford, program manager of the Defense Test Resource Management Center's (DTRMC) Test and Evaluation/Science and Technology (T&E/S&T) program, for funding this effort under the hypersonic test focus area.

References

[1] Eklund, D. R., Baurle, R. A., and Gruber, M. R., "Numerical Study of a Scramjet Combustor Fueled by an Aerodynamic Ramp Injector in Dual-Mode Combustion," AIAA Paper 2001-0379, Jan. 2001.

[2] Xiao, X., Edwards, J. R., Hassan, H. A., and Cutler, A. D., "Variable Turbulent Schmidt Number Formulation for Scramjet Applications," *AIAA Journal*, Vol. 44, No. 3, 2006, pp. 593–599.

[3] Cutler, A. D., Carty, A. A., Doemer, S. E., Diskin, G. S., and Drummond, J. P., "Supersonic Coaxial Jet Flow Experiment for CFD Validation," AIAA Paper 1999-3388, July 1999.

[4] Burrows, M. C., and Kurkov, A. P., "Analytical and Experimental Study of Supersonic Combustion of Hydrogen in a Vitiated Airstream," NASA TM X-2828, Sept. 1973.

[5] Xiao, X., Edwards, J. R., Hassan, H. A., and Gaffney Jr, R. L., "Role of Turbulent Prandtl Number on Heat Flux at Hypersonic Mach Numbers," AIAA Paper 2005-1098, Jan. 2005.

[6] Keistler, P. G., Gaffney Jr, R. L., Xiao, X., and Hassan, H. A., "Turbulence Modeling for Scramjet Applications," AIAA Paper 2005-5382, June 2005.

[7] Girimaji, S. S., "Simple Recipe for Modeling Reaction-Rates in Flows with Turbulent-Combustion," AIAA Paper 1991-1792, June 1991.

[8] Baurle, R. A., Hsu, A. T., and Hassan, H. A., "Assumed and Evolution Probability Density Functions in Supersonic Turbulent Combustion Calculations," *Journal of Propulsion and Power*, Vol. 11, No. 6, 1995, pp. 1132–1138.

[9] Jachimowski, C. J., "An Analytic Study of the Hydrogen-Air Reaction Mechanism with Application to Scramjet Combustion," NASA Technical Paper 2791, Feb. 1988.

[10] Connaire, M. O., Curran, H. J., Simmie, J. M., Pitz, W. J., and Westbrook, C. K., "A Comprehensive Modeling Study of Hydrogen Oxidation," *International Journal of Chemical Kinetics*, Vol. 36, No. 11, 2004, pp. 603–622.

[11] Brinckman, K. W., Calhoon Jr., W. H., Mattick, S. J., Tomes, J., and Dash, S. M., "Scalar Variance Model Validation for High-Speed Variable Composition Flows," AIAA Paper 2006-0715, Jan. 2006.

[12] Calhoon Jr., W. H., Brinckman, K. W., Tomes, J., Mattick, S. J., and Dash, S. M., "Scalar Fluctuations and Transport Modeling for Application to High-Speed Reacting Flows," AIAA Paper 2006-1452, Jan. 2006.

[13] Robinson, D. F., and Hassan, H. A., "Further Development of the k-ζ (Enstrophy) Turbulence Closure Model," *AIAA Journal*, Vol. 36, No. 10, 1998, pp. 1825–1833.

[14] Launder, B. E., "Heat and Mass Transport," *Turbulent Topics in Applied Physics*, edited by P. Bradshow, Springer–Verlag, Berlin, Vol. 12, 1978.
[15] Edwards, J. R., "Advanced Implicit Algorithm for Hydrogen-Air Combustion Calculation," AIAA Paper 1996-3129, June 1996.
[16] Edwards, J. R., "A Low Diffusion Flux Splitting Scheme for Navier–Stokes Calculations," *Computers and Fluids*, Vol. 26, No. 6, 1997, pp. 635–659.

P. Givi
Associate Editor